MRI correlates of neurofibrillary tangle pathology at autopsy

A voxel-based morphometry study

J.L. Whitwell, PhD
K.A. Josephs, MST, MD, MS
M.E. Murray, BS
K. Kantarci, MD
S.A. Przybelski, BS
S.D. Weigand, MS
P. Vemuri, PhD
M.L. Senjem, BS
J.E. Parisi, MD
D.S. Knopman, MD
B.F. Boeve, MD
R.C. Petersen, PhD, MD
D.W. Dickson, MD
C.R. Jack, Jr., MD

Address correspondence and reprint requests to Dr. Clifford R. Jack, Jr., Department of Radiology, Mayo Clinic, 200 First St. SW, Rochester, MN 55905
jack.clifford@mayo.edu

ABSTRACT

Background: Neurofibrillary tangles (NFTs), composed of hyperphosphorylated tau proteins, are one of the pathologic hallmarks of Alzheimer disease (AD). We aimed to determine whether patterns of gray matter atrophy from antemortem MRI correlate with Braak staging of NFT pathology.

Methods: Eighty-three subjects with Braak stage III through VI, a pathologic diagnosis of low- to high-probability AD, and MRI within 4 years of death were identified. Voxel-based morphometry assessed gray matter atrophy in each Braak stage compared with 20 pathologic control subjects (Braak stages 0 through II).

Results: In pairwise comparisons with Braak stages 0 through II, a graded response was observed across Braak stages V and VI, with more severe and widespread loss identified at Braak stage VI. No regions of loss were identified in Braak stage III or IV compared with Braak stages 0 through II. The lack of findings in Braak stages III and IV could be because Braak stage is based on the presence of any NFT pathology regardless of severity. Actual NFT burden may vary by Braak stage. Therefore, tau burden was assessed in subjects with Braak stages 0 through IV. Those with high tau burden showed greater gray matter loss in medial and lateral temporal lobes than those with low tau burden.

Conclusions: Patterns of gray matter loss are associated with neurofibrillary tangle (NFT) pathology, specifically with NFT burden at Braak stages III and IV and with Braak stage itself at higher stages. This validates three-dimensional patterns of atrophy on MRI as an approximate in vivo surrogate indicator of the full brain topographic representation of the neurodegenerative aspect of Alzheimer disease pathology. ***Neurology*® 2008;71:743–749**

GLOSSARY

AD = Alzheimer disease; **AGD** = argyrophilic grains disease; **aMCI** = amnestic mild cognitive impairment; **CDR-SB** = Clinical Dementia Rating scale sum of boxes; **DLB** = dementia with Lewy bodies; **FDR** = false-discovery rate; **MMSE** = Mini-Mental State Examination; **NFT** = neurofibrillary tangle; **NIA** = National Institute on Aging; **SPGR** = spoiled gradient echo; **VBM** = voxel-based morphometry.

The presence of neurofibrillary tangles (NFTs), composed of hyperphosphorylated tau proteins, and amyloid plaques are pathologic hallmarks of Alzheimer disease (AD). The topographic distribution and progression of NFT pathology in AD has been described by Braak and Braak and divided into six distinct stages.[1] NFTs first appear in the transentorhinal region, before spreading to other regions of the medial temporal lobes and then to the neocortical association areas and subcortical nuclei.[1]

From the Departments of Radiology (J.L.W., K.K., P.V., C.R.J.), Neurology (Behavioral Neurology) (K.A.J., D.S.K., B.F.B., R.C.P.), Biostatistics (S.A.P., S.D.W.), Information Technology (M.L.S.) and Laboratory Medicine and Pathology (J.E.P.), Mayo Clinic, Rochester, MN; and Department of Neuroscience (Neuropathology) (M.E.M., D.W.D.), Mayo Clinic, Jacksonville, FL.

Supported by grants P50 AG16574, U01 AG06786, and R01 AG11378 from the National Institute on Aging (NIA), Bethesda, MD; the NIH Roadmap Multidisciplinary Clinical Research Career Development Award Grant (K12/NICHD)-HD49078; the Robert H. and Clarice Smith and Abigail Van Buren Alzheimer's Disease Research Program; the Paul B. Beeson Career Development Award in Aging K23 AG030935 from the NIH/NIA; the Alexander Family Alzheimer's Disease Research Professorship of the Mayo Foundation, USA; and the NIH Construction Grant (NIH C06 RR018898).

Disclosure: D.S.K. has been a consultant to GE HealthCare, GlaxoSmithKline, and Myriad Pharmaceuticals; has served on a Data Safety Monitoring Board for Neurochem Pharmaceuticals; and is an investigator in a clinical trial sponsored by Elan Pharmaceuticals. R.C.P. has been a consultant to GE Healthcare and is on a Treatment Effects Monitoring Committee for a clinical trial sponsored by Elan Pharmaceuticals. B.F.B. is an investigator in a clinical trial sponsored by Myriad Pharmaceuticals. C.R.J. receives research support from Pfizer in the form of research grants.

MRI studies have demonstrated patterns of atrophy that seem to match the progression of NFTs in subjects with AD, with early involvement of medial temporal lobe,[2,3] and more widespread temporoparietal neocortical loss as subjects progress.[4-7] However, these studies did not have pathologic confirmation and therefore can only imply an association between the progression of atrophy and NFT pathology. A few studies have looked specifically at autopsied subjects and found correlations between Braak NFT stage (hereafter referred to as Braak stage) or NFT density and hippocampal volume,[8-11] as well as rates of brain atrophy.[12] These studies were region-of-interest–based studies, however, and therefore do not allow an assessment of correlations between NFT stage/severity and the full three-dimensional representation of gray matter loss on MRI. The aim of this study was to use the technique of voxel-based morphometry (VBM), which assesses patterns of atrophy across the whole brain, to examine the relationship between patterns of gray matter atrophy and the Braak staging scheme.

METHODS

Subject selection. Subjects were identified from the neuropathology files of the Mayo Clinic. All subjects had been studied prospectively in the Mayo Clinic Alzheimer's Disease Research Center or Alzheimer's Disease Patient Registry during life and had undergone autopsy. All subjects underwent annual clinical evaluations and cognitive testing, including the Mini-Mental State Examination (MMSE)[13] and Clinical Dementia Rating scale sum of boxes (CDR-SB).[14] The diagnosis of dementia was made based on the *Diagnostic and Statistical Manual of Mental Disorders*, Fourth Edition,[15] and the diagnosis of AD was made based on National Institute of Neurological and Communicative Disorders and Stroke–Alzheimer's Disease and Related Disorders Association criteria.[16] Clinical diagnosis of amnestic mild cognitive impairment was made according to the criteria by Petersen et al.[17,18] Informed consent was obtained for participation in the studies, which were approved by the Mayo Institutional Review Board. Apolipoprotein E testing was also performed in all subjects as previously described.[19]

Subjects were identified if they had a pathologic diagnosis along the normal to AD spectrum, i.e., Braak stages 0 through VI and low-, intermediate-, or high-likelihood AD according to the National Institute on Aging (NIA)–Reagan criteria.[20] Subjects were excluded if they had pathologic evidence of hippocampal sclerosis or another neurodegenerative disorder, except Lewy body disease and argyrophilic grain disease because neither is associated with widespread cerebral atrophy.[21,22] The clinical histories of all cases were reviewed, and subjects who had a clinical diagnosis of a non-AD dementia, had received treatments, or had concurrent illnesses interfering with cognitive function were excluded.

From this group, we selected all subjects with Braak stage III or VI who had an MRI within 4 years of death. The requirement that the MRI occur within 4 years of death serves to reduce uncertainty about pathologic progression between MRI and death. To identify patterns of cerebral loss in subjects with each of these Braak stages, we selected a group of subjects that we labeled pathologically "normal." These were subjects with Braak stage 0, I, or II who had an MRI. Braak stages 0 through II have been considered as low limbic stages with pathologic changes consistent with typical aging.[23] We used the earliest MRI available in these controls to minimize the degree of NFT pathology in the brain at the time of the MRI. We excluded from the pathologic control group potential subjects who had been given a clinical diagnosis of dementia. All MRIs were reviewed, and scans were rejected for poor quality (e.g., motion artifacts) or the presence of other pathologies (e.g., large cortical infarcts) that might influence the structural analysis. We identified 83 subjects with Braak stage III through VI with an MRI within 4 years of death, and 20 subjects who met criteria for the pathologic control group.

Pathologic assessment. Neuropathologic examinations were performed according to the recommendations of the Consortium to Establish a Registry for Alzheimer's Disease.[24] In all cases, pathologic assessment and diagnosis was conducted by one or both of two expert neuropathologists (D.W.D. or J.E.P.). After removal, the brain was divided into right and left hemibrains. The left hemibrain was fixed, sectioned, and then stained as previously described.[25] Each specimen was assigned to Braak stages I through VI based on the earliest appearance of neurofibrillary pathology, which was operationalized as follows: stage I, NFT confined to transentorhinal cortex (layer IV); stage II, NFT in entorhinal cortex (layer II); stage III, NFT in hippocampus (CA1 and subiculum); stage IV, NFT in temporal lobe association neocortex (mild); stage V, NFT in temporal association neocortex (moderate to severe); and stage VI, NFT in temporal association neocortex (severe) and primary visual cortex.[1] Braak stage 0 was assigned in the absence of NFT. AD was diagnosed based on NIA–Reagan criteria as low-, intermediate-, or high-probability AD.[20] The presence of argyrophilic grains[26] was recorded, and Lewy bodies were assessed with α-synuclein immunostaining according to established criteria.[27] The likelihood that the pathologic findings are associated with dementia with Lewy bodies was assigned according to criteria.[27]

Tau burden analysis. As will be shown, we did not find a relationship between Braak stage and gray matter loss in Braak stages II through IV relative to Braak stages 0 through II. For this reason, we also assessed the actual burden of NFT deposition by measuring tau quantitatively. A strong correlation has previously been observed between tau-labeled NFT density and silver-stained NFT density in the limbic cortices.[28] To obtain a quantitative measure of tau burden, an unbiased computer-assisted image analyzer was used to quantify the percentage area occupied by tau in all subjects with Braak stage IV or less who had available tissue slides (n = 36). A section of CA1, subiculum, parahippocampal gyrus, and occipitotemporal gyrus was traced and analyzed using Image Scope software (Aperio, Vista, CA). A monoclonal tau antibody, CP13, was used to detect NFTs and neuropil threads (epitope phosphor-serine 202) at a dilution of 1:100.[29] A percent positivity/area traced was obtained using an algorithm (positive pixel count) that detects the chromogen DAB in the anti-mouse 2° antibody. The Dako Cytomation Envision kit was used on the Dako Universal Autostainer (Dako, Carpinteria, CA). The tau burdens in each of the four regions

Table Subject demographics and clinicopathologic classifications for all subjects by Braak stage

	Controls, Braak stage 0–II (n = 20)	Braak stage			
		III (n = 10)	IV (n = 13)	V (n = 32)	VI (n = 27)
No. of women (%)	12 (60)	7 (70)	6 (46)	18 (56)	18 (67)
No. of APOE ε4 carriers (%)*	4 (20)	6 (60)	5 (38)	16 (52)	17 (68)
Education, y, median (range)	15 (9–20)	11 (7–18)	16 (8–18)	15 (8–20)	15 (8–18)
Age at scan, y,* median (range)	80 (53–93)	90 (81–100)	86 (72–93)	86 (59–98)	81 (49–92)
Age at death, y,* median (range)	88 (57–99)	92 (81–103)	88 (74–94)	87 (60–100)	83 (51–94)
Time from scan to death, y,† median (range)	4.8 (0.1–13.5)	1.7 (0.1–4.0)	1.6 (0.8–3.9)	1.8 (0.2–4.0)	2.3 (0.6–3.9)
MMSE score, /30,† median (range)	28 (24–30)	26 (18–30)	27 (19–30)	22 (12–29)	14 (7–29)
CDR-SB, /18,† median (range)	0.0 (0–0.5)	2.3 (0–6.0)	0.0 (0–17.0)	7.0 (0–18.0)	10.0 (1.5–18.0)
Clinical diagnosis at MRI, normal/aMCI/AD (%)	20/0/0 (100/0/0)	3/3/4 (30/30/40)	7/3/3 (54/23/23)	5/5/22 (16/16/68)	0/1/26 (0/4/96)
Clinical diagnosis at death, normal/aMCI/AD (%)	17/3/0 (85/15/0)	3/3/4 (30/30/40)	7/3/3 (54/23/23)	5/3/24 (16/9/75)	0/0/27 (0/0/100)
NIA–Reagan probability of AD, low/intermediate/high (%)	20/0/0 (100/0/0)	6/3/1 (60/30/10)	8/4/1 (62/31/7)	1/4/27 (3/13/84)	0/1/26 (0/4/96)
McKeith probability of DLB, low/intermediate/high (%)	0	0	0	2/6/2‡ (6/19/6)	2/3/0‡ (7/11/0)
AGD present (%)	6 (30)	3 (30)	2 (15)	3 (9)	0

Significant differences across groups at *$p < 0.05$, †$p < 0.001$.
‡One additional subject had Lewy body pathology confined to the amygdala.
MMSE = Mini-Mental State Examination; CDR-SB = Clinical Dementia Rating scale sum of boxes; aMCI = amnestic mild cognitive impairment; AD = Alzheimer disease; NIA = National Institute on Aging; DLB = dementia with Lewy bodies; AGD = argyrophilic grains disease.

were averaged to generate an average tau burden for each subject.

Image analysis. T1-weighted coronal spoiled gradient echo (SPGR) images were acquired as previously described.[7] An optimized method of VBM was applied, implemented using SPM2 (http://www.fil.ion.ucl.ac.uk/spm).[30,31] The processing steps were performed as previously described.[7,31] Briefly, all SPGR images were normalized to a customized template created from all subjects in the study. The spatial normalization was optimized by normalizing the gray matter images to the customized gray matter template. Images were segmented using customized prior probability maps, modulated, and smoothed with an 8-mm full-width at half-maximum smoothing kernel.

Group-wise comparisons were performed between each Braak stage (i.e., III, IV, V, or VI) and the pathologic control group (Braak stages 0 through II) using a single-subject condition and covariates model, including age and sex as nuisance variables (corrected for multiple comparisons using the false-discovery rate [FDR], $p < 0.005$). Group analyses were also performed between subjects with a high tau burden (10% or greater) and a low tau burden (less than 10%) within subjects with Braak stage IV or less who had tau burden measurements, including age and sex as nuisance variables. Given the smaller number of subjects assessed, a more lenient statistical threshold of $p < 0.005$ uncorrected for multiple comparisons was applied.

Statistical analysis. Kruskal–Wallis tests were used to compare groups on age at time of scan, years of education, time from scan to death, MMSE, and CDR-SB. The Fisher exact test was used to compare groups on sex and the proportion of APOE ε4 carriers. Spearman rank correlation was used to assess the relationship between Braak stage and average tau burden. We report medians and use nonparametric methods because of skewness in the numeric clinical variables.

RESULTS

Subject demographics. The subject demographics are shown in the table. There was a difference across groups in the age at scan ($p = 0.002$) and age at death ($p = 0.02$). The APOE ε4 frequency differed across groups ($p = 0.02$), with the lowest frequency observed in the pathologic controls. There was also a difference in the time from scan to death ($p < 0.001$) because of the longer time interval allowed for the pathologic controls. The cognitive measures worsened with increasing Braak stage ($p < 0.001$ for both).

Braak stage analysis. The Braak stage VI group showed a widespread pattern of gray matter loss relative to pathologic controls (corrected FDR, $p <$

Figure 1 Patterns of gray matter loss on MRI in subjects with Braak stage III to IV, V, or VI when compared with the pathologic control group*

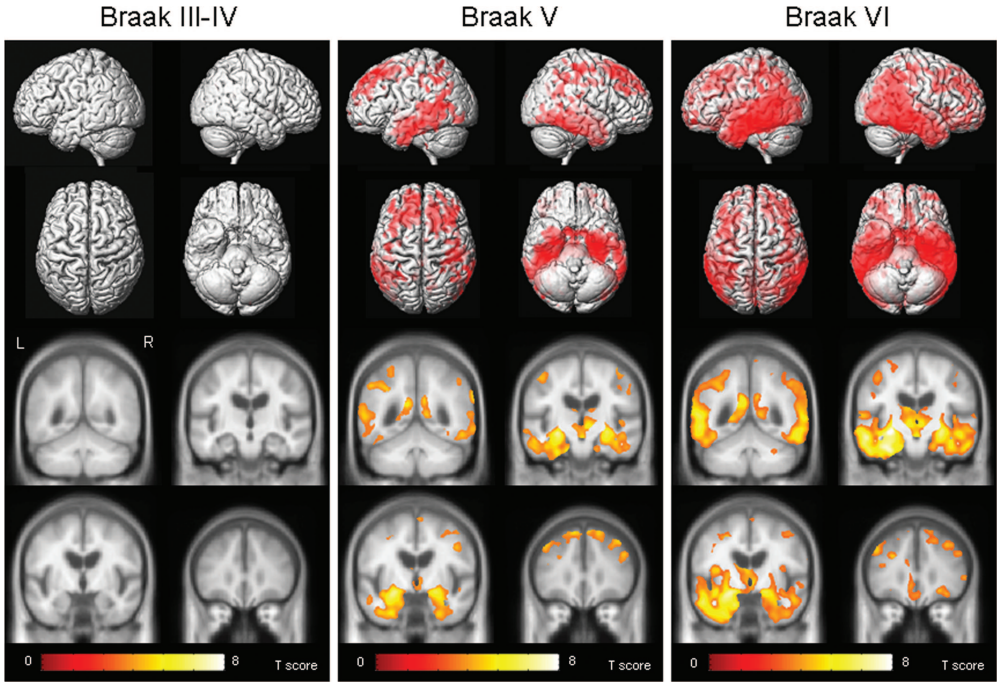

*Corrected for multiple comparisons, false-discovery rate, $p < 0.005$. The patterns of cortical atrophy are shown on a three-dimensional surface render (top). In addition, the results are shown on representative coronal slices through the customized template (coordinates: y = −50, −15, −5, 35; bottom).

0.005; figure 1). Loss was observed throughout the temporal lobes, including medial temporal regions, such as amygdala, hippocampus, entorhinal cortex, and adjacent parahippocampal gyrus, as well as inferior, middle, and superior temporal gyri, fusiform gyrus, and the anterior temporal pole. A left-greater-than-right asymmetry was observed in the temporal lobe. The posterior temporal lobe and temporoparietal neocortex were also heavily involved. Loss was also observed bilaterally in inferior, middle, and superior frontal lobes, as well as orbitofrontal cortex, posterior cingulate, precuneus, anterior cingulate, basal forebrain, and insula. Gray matter loss was also observed in the occipital lobe, including the superior bank of the primary visual cortex. Subcortical gray matter loss was observed in thalamus, hypothalamus, head of the caudate nucleus, and posterior putamen.

The Braak stage V group showed a pattern of gray matter loss affecting the medial temporal lobes, including amygdala, hippocampus, entorhinal cortex, and adjacent parahippocampal gyrus. The fusiform gyrus and inferior and middle temporal lobes were also involved, with a relative sparing of the anterior superior temporal gyrus (corrected FDR, $p < 0.005$; figure 1). Gray matter loss extended back into posterior temporal lobe, involving the entire extent of the hippocampus. The medial temporal lobe loss was bilateral, with slightly greater loss in the left hemisphere. Gray matter loss was also identified throughout the parietal lobe and the posterior cingulate, with some minor involvement of the precuneus. The frontal lobes, particularly the middle and superior frontal gyri, and the basal forebrain were also involved. Subcortical gray matter loss was only identified in the thalamus and hypothalamus.

No regions of gray matter loss were observed with Braak stages III or IV when each was individually compared with the pathologic control group (FDR, $p < 0.005$). The number of subjects in each of these groups was small, however; therefore, the Braak stage III and IV groups were combined into one larger group of 27 subjects and compared with controls. Again, no regions of gray matter loss were identified (figure 1). At an even more lenient threshold of $p < 0.005$ uncorrected for multiple comparisons, no coherent pattern of gray matter loss was observed.

Tau burden analysis. Tau burden was significantly correlated to Braak stage (Spearman rank correlation = 0.8, $p < 0.001$), although it is clear that tau burden varies to a large degree in each Braak stage (figure 2). The subjects with a high tau burden (≥10%) showed a pattern of gray matter loss affecting the hippocampus, parahippocampal gyrus, and lateral temporal lobes compared with subjects with a low tau burden (<10%) (figure 3).

Figure 2 **Relationship between tau burden and Braak stage in the 36 subjects with Braak stage 0 through IV**

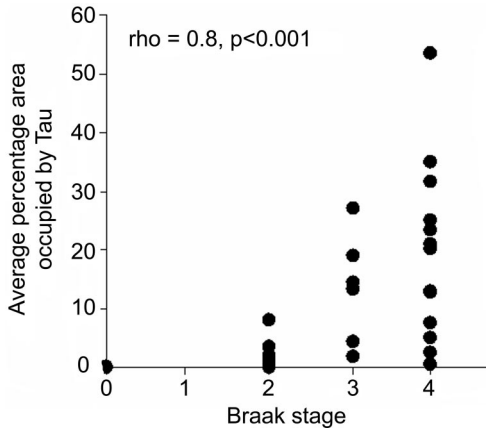

DISCUSSION This study examines the relationship between three-dimensional patterns of gray matter loss and NFT pathology in subjects with various degrees of AD-type pathology in their brain. The results showed a dichotomy across the Braak spectrum, with subjects with Braak stages V and VI showing widespread patterns of gray matter loss, whereas no regions of gray matter loss were identified in Braak stages III and IV.

The subjects with Braak stage VI showed a widespread pattern of loss, involving temporal, parietal, and frontal lobes, basal forebrain, posterior cingulate, precuneus, anterior cingulate, insula, and subcortical nuclei. The occipital lobe was also involved, including the primary visual cortex. The patterns of loss were somewhat asymmetric, with the left hemisphere showing greater loss than the right. However, it would be unwise to draw any conclusions regarding the laterality of AD from these results because this study is biased by the fact that only the left side of the brain was sampled in the pathologic analysis, in contrast to VBM, which assesses loss throughout the brain. The subjects with Braak stage V showed a less severe and widespread pattern of loss. The temporal, frontal, and parietal lobes were involved, although there was a lack of involvement of the insula, orbitofrontal cortex, putamen, caudate nuclei, and primary visual cortex. The distribution of loss across these two groups matches relatively well with the distribution of NFT at Braak stages V and VI.[1] However, we did not identify gray matter loss in the insula and orbitofrontal cortex at Braak stage V even though they can be involved pathologically.[1]

In contrast, subjects with Braak stage III or IV showed no regions of gray matter loss compared with controls when analyzed separately or together as a larger group. A study looking at cerebral perfusion using single photon emission tomography similarly found a much greater degree of medial temporal, temporoparietal, and frontal defects in subjects with Braak stage V or VI compared with those with Braak stages I through IV.[32] The majority of subjects in our study with Braak stage V or VI also had a clinical diagnosis of AD at their MRI scan (81%), whereas only 30% of those with Braak stage III or IV had a clinical diagnosis of AD. Likewise, the APOE $\varepsilon 4$ allele frequency was somewhat higher in subjects with Braak stage V or VI (56%), compared with those with Braak stage III or IV (48%). The fact that Braak stages III and IV clustered together with little evident gray matter loss, whereas noticeable changes in VBM pattern were observed at higher Braak stages, suggests that the change in the magnitude of NFT load between successive lower Braak stages is smaller than the corresponding change in NFT load between higher Braak stages. Therefore, while Braak staging is monotonic, it is nonlinear across the entire I to VI range.

However, the finding of no gray matter loss in Braak stages III and IV is somewhat unexpected because neurofibrillary changes are found in the entorhinal cortex, hippocampus, and amygdala during these Braak stages,[1] and one might expect to see con-

Figure 3 **Patterns of gray matter loss on MRI in subjects with Braak stage 0 through IV and high tau burden (≥10%) compared with subjects with Braak stage 0 through IV and low tau burden (<10%)**

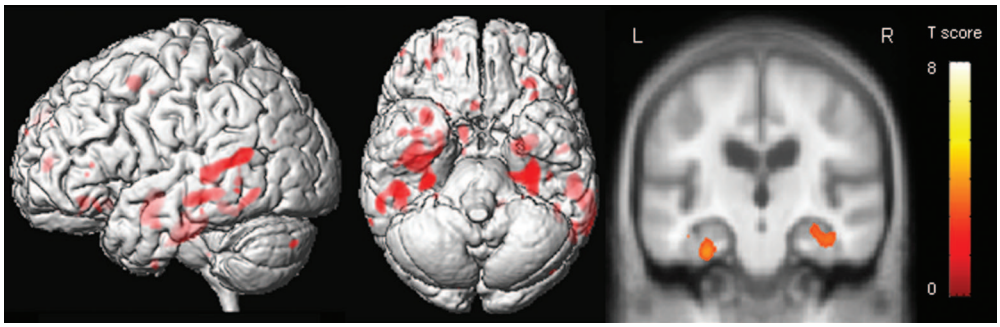

The patterns of atrophy are shown on a three-dimensional surface render and on a representative coronal slice through the temporal lobe.

comitant gray matter loss. There are a number of possible explanations for this discordance. One such explanation could be that the degree of gray matter loss could be more closely related to the actual NFT burden. Braak staging is based on the presence of any NFT in a certain region, not quantitative NFT load, and therefore, while Braak stage may correlate to NFT burden, variation in NFT burden among subjects of the same Braak stage may occur. To test this hypothesis, we measured the degree of tau burden in each of the subjects with Braak stages 0 through IV. It was clear that the tau burden varied to a large degree within each Braak stage. For example, subjects in each Braak stage from 0 through IV (except Braak I, where there was no data) were found in the low (<10%) tau burden group. We also found that the subjects with high tau burden showed greater gray matter loss in the medial and lateral temporal lobes than the subjects with low tau burden. This result therefore demonstrates that gray matter loss in these regions was present in some of the subjects with Braak stage IV or less, and that this loss correlates better to the actual tau burden than the Braak stage in these subjects. A previous pathologic study has similarly demonstrated a close relationship between NFT density and degree of neuronal loss and has shown that the NFT density varies across subjects with the same Braak stages.[33]

It is also possible, however, that the degree of gray matter loss could be influenced by other factors, such as the presence of amyloid plaques in the brain. However, the topography of gray matter loss observed in Braak stages V and VI matches the topography of NFT distribution and does not match the topography of amyloid distribution.[1] The conclusion we draw, therefore, is that the appropriate pathologic correlate of gray matter loss in AD is tangles, not plaques. A previous study has in fact shown that the rate of brain volume loss on serial MRI correlates with Braak stage and not amyloid burden.[12] The degree of vascular burden could also influence the relationship between pathology, gray matter loss, and clinical phenotype.[34]

A limitation of our study is that the MRI scans were not performed at the time of death, but an average of 2 years before death in the subjects with Braak stages III through VI. It is therefore possible that further gray matter loss could have occurred between the time of MRI and the time of death. It is also possible that the Braak stage at the time of scan may have been lower than that reported at death, although it has been suggested that progression from low to high Braak stages can take decades.[23,35]

This study therefore provides evidence that patterns of gray matter loss are associated with the presence of NFTs in the brain. At Braak stages III and IV, the tau burden seems to play an important role in determining the pattern of brain loss, whereas Braak stage, which is only an indirect measure of burden, is less associated with the degree of brain loss. Subjects with Braak stage V or VI show severe patterns of atrophy, which are associated with Braak stage itself. We assume that at high stages, the much larger NFT burden overwhelms case-to-case inconsistency in the relationship between burden and stage, thus accounting for the good correlation between MRI atrophy and Braak stage. These results validate three-dimensional patterns of atrophy on MRI as an approximate in vivo surrogate indicator of the full brain topographic representation of the neurodegenerative aspect of AD pathology.

AUTHOR CONTRIBUTIONS

Statistical analysis was performed by S.A.P. and S.D.W.

Received September 17, 2007. Accepted in final form May 29, 2008.

REFERENCES

1. Braak H, Braak E. Neuropathological stageing of Alzheimer-related changes. Acta Neuropathol (Berl) 1991; 82:239–259.
2. Fox NC, Warrington EK, Freeborough PA, et al. Presymptomatic hippocampal atrophy in Alzheimer's disease: a longitudinal MRI study. Brain 1996;119(pt 6): 2001–2007.
3. Jack CR Jr, Petersen RC, Xu YC, et al. Prediction of AD with MRI-based hippocampal volume in mild cognitive impairment. Neurology 1999;52:1397–1403.
4. Fox NC, Crum WR, Scahill RI, et al. Imaging of onset and progression of Alzheimer's disease with voxel-compression mapping of serial magnetic resonance images. Lancet 2001;358:201–205.
5. Matsuda H, Kitayama N, Ohnishi T, et al. Longitudinal evaluation of both morphologic and functional changes in the same individuals with Alzheimer's disease. J Nucl Med 2002;43:304–311.
6. Chetelat G, Landeau B, Eustache F, et al. Using voxel-based morphometry to map the structural changes associated with rapid conversion in MCI: a longitudinal MRI study. Neuroimage 2005;27:934–946.
7. Whitwell JL, Przybelski S, Weigand SD, et al. 3D maps from multiple MRI illustrate changing atrophy patterns as subjects progress from MCI to AD. Brain 2007;130(pt 7):1777–1786.
8. Jack CR Jr, Dickson DW, Parisi JE, et al. Antemortem MRI findings correlate with hippocampal neuropathology in typical aging and dementia. Neurology 2002;58:750–757.
9. Gosche KM, Mortimer JA, Smith CD, et al. Hippocampal volume as an index of Alzheimer neuropathology: findings from the Nun Study. Neurology 2002;58:1476–1482.
10. Csernansky JG, Hamstra J, Wang L, et al. Correlations between antemortem hippocampal volume and postmortem neuropathology in AD subjects. Alzheimer Dis Assoc Disord 2004;18:190–195.

11. Silbert LC, Quinn JF, Moore MM, et al. Changes in premorbid brain volume predict Alzheimer's disease pathology. Neurology 2003;61:487–492.
12. Josephs KA, Whitwell JL, Ahmed Z, et al. β-Amyloid burden is not associated with rates of brain atrophy. Ann Neurol 2007;63:204–212.
13. Folstein MF, Folstein SE, McHugh PR. "Mini-Mental State": a practical method for grading the cognitive state of patients for the clinician. J Psychiatr Res 1975;12:189–198.
14. Hughes CP, Berg L, Danziger WL, et al. A new clinical scale for the staging of dementia. Br J Psychiatry 1982;140:566–572.
15. American Psychiatric Association. Diagnostic and Statistical Manual of Mental Disorders, 4th ed. Washington, DC: American Psychiatric Association, 1994.
16. McKhann G, Drachman D, Folstein M, et al. Clinical diagnosis of Alzheimer's disease: report of the NINCDS-ADRDA Work Group under the auspices of Department of Health and Human Services Task Force on Alzheimer's Disease. Neurology 1984;34:939–944.
17. Petersen RC, Smith GE, Waring SC, et al. Mild cognitive impairment: clinical characterization and outcome. Arch Neurol 1999;56:303–308.
18. Petersen RC. Mild cognitive impairment as a diagnostic entity. J Intern Med 2004;256:183–194.
19. Crook R, Hardy J, Duff K. Single-day apolipoprotein E genotyping. J Neurosci Methods 1994;53:125–127.
20. Hyman BT, Trojanowski JQ. Consensus recommendations for the postmortem diagnosis of Alzheimer's disease. The National Institute on Aging, and Reagan Institute Working Group on Diagnostic Criteria for the Neuropathological Assessment of Alzheimer's Disease. Neurobiol Aging 1997;18:S1–S2.
21. Josephs KA, Whitwell JL, Parisi JE, et al. Argyrophilic grains: a distinct disease or an additive pathology? Neurobiol Aging 2008;29:566–573.
22. Whitwell JL, Weigand SD, Shiung MM, et al. Focal atrophy in dementia with Lewy bodies on MRI: a distinct pattern from Alzheimer's disease. Brain 2007;130:708–719.
23. Mesulam MM. Aging, Alzheimer's disease, and dementia. In: Mesulam MM, ed. Principles of Behavioral and Cognitive Neurology, 2nd ed. Oxford: Oxford University Press, 2000.
24. Mirra SS, Heyman A, McKeel D, et al. The Consortium to Establish a Registry for Alzheimer's Disease (CERAD), part II: standardization of the neuropathologic assessment of Alzheimer's disease. Neurology 1991;41:479–486.
25. Knopman DS, Parisi JE, Salviati A, et al. Neuropathology of cognitively normal elderly. J Neuropathol Exp Neurol 2003;62:1087–1095.
26. Braak H, Braak E. Cortical and subcortical argyrophilic grains characterize a disease associated with adult onset dementia. Neuropathol Appl Neurobiol 1989;15:13–26.
27. McKeith IG, Dickson DW, Lowe J, et al. Diagnosis and management of dementia with Lewy bodies: third report of the DLB Consortium. Neurology 2005;65:1863–1872.
28. Nakano H, Kobayashi K, Sugimori K, et al. Regional analysis of differently phosphorylated tau proteins in brains from patients with Alzheimer's disease. Dement Geriatr Cogn Disord 2004;17:122–131.
29. Jicha GA, Bowser R, Kazam IG, Davies P. Alz-50 and MC-1, a new monoclonal antibody raised to paired helical filaments, recognize conformational epitopes on recombinant tau. J Neurosci Res 1997;48:128–132.
30. Ashburner J, Friston KJ. Voxel-based morphometry: the methods. Neuroimage 2000;11:805–821.
31. Senjem ML, Gunter JL, Shiung MM, et al. Comparison of different methodological implementations of voxel-based morphometry in neurodegenerative disease. Neuroimage 2005;26:600–608.
32. Bradley KM, O'Sullivan VT, Soper ND, et al. Cerebral perfusion SPET correlated with Braak pathological stage in Alzheimer's disease. Brain 2002;125:1772–1781.
33. Mizuno Y, Ikeda K, Tsuchiya K, et al. Two distinct subgroups of senile dementia of Alzheimer type: quantitative study of neurofibrillary tangles. Neuropathology 2003;23:282–289.
34. Schneider JA, Boyle PA, Arvanitakis Z, et al. Subcortical infarcts, Alzheimer's disease pathology, and memory function in older persons. Ann Neurol 2007;62:59–66.
35. Braak H, Braak E. Evolution of the neuropathology of Alzheimer's disease. Acta Neurol Scand Suppl 1996;165:3–12.